

Supporting Information

Organic Fluorine Mediated Intermolecular Interactions: Insights from Experimental and Theoretical Charge Density Analyses

Sakshi,^{a,#} Yogita Gupta,^{b,#} Craig M. Robertson,^c Parthapratim Munshi,^{b,*} and Angshuman Roy Choudhury^{a,*}

^aDepartment of Chemical Sciences, Indian Institute of Science Education and Research, Mohali, Knowledge City, Sector 81, S. A. S. Nagar, Manauli PO, Mohali. Punjab. 140306, India.

^bMultifunctional Molecular Materials Laboratory, Department of Chemistry, School of Natural Sciences, Shiv Nadar Institution of Eminence Deemed to be University, Delhi NCR, Uttar Pradesh. 201314, India

^cDepartment of Chemistry, University of Liverpool, Crown Street, Liverpool, L69 7ZD (UK)

#contributed equally

E-mail: angshurc@iisermohali.ac.in, parthapratim.munshi@snu.edu.in

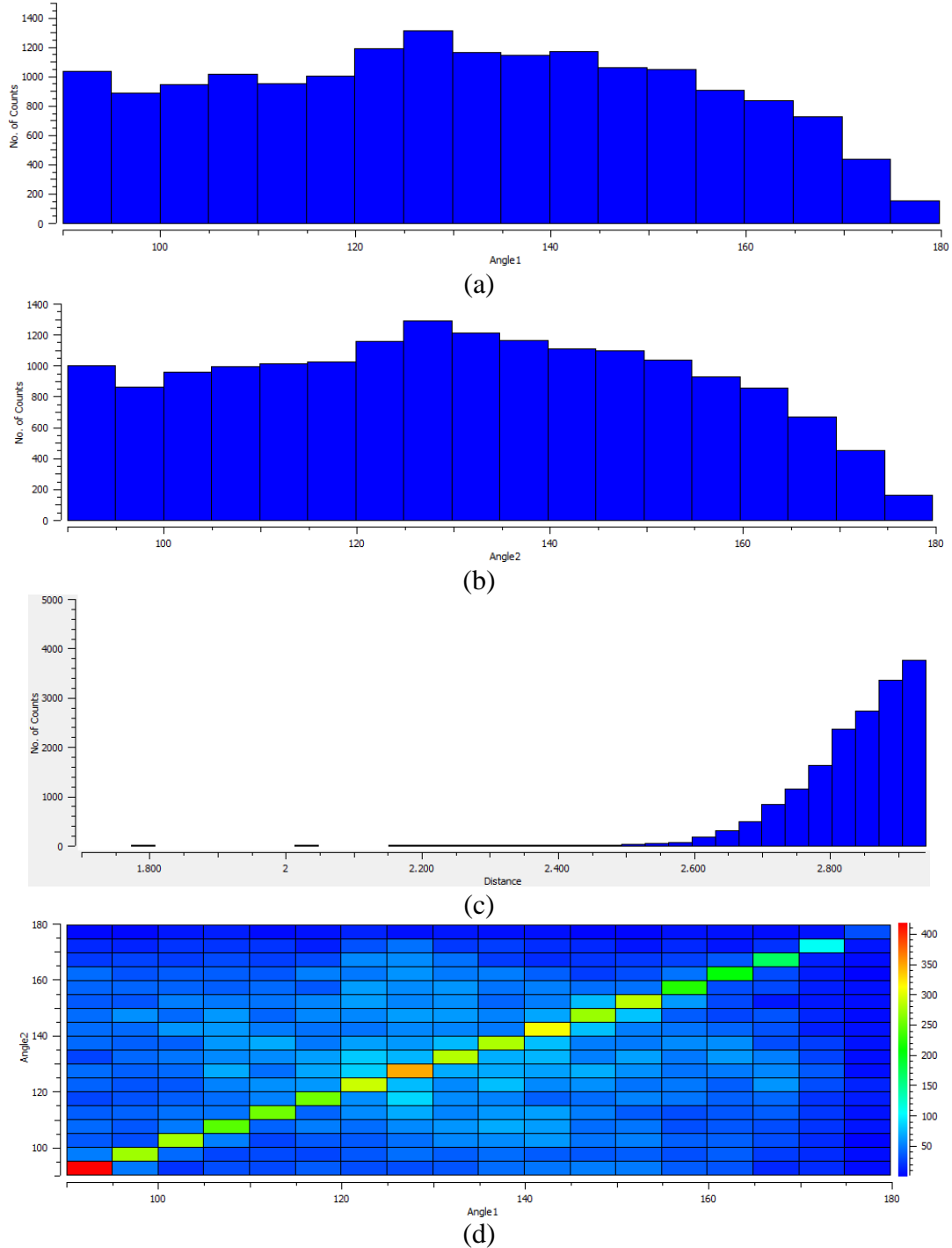


Figure S1: (a) Histogram for angle 1 (θ_1), (b) Histogram for angle 2 (θ_2), (c) Distance histogram, and (d) Heat plot for angle (θ_1 and θ_2), for all the structures having C–F···F–C interaction along with other intermolecular interactions (search 1).

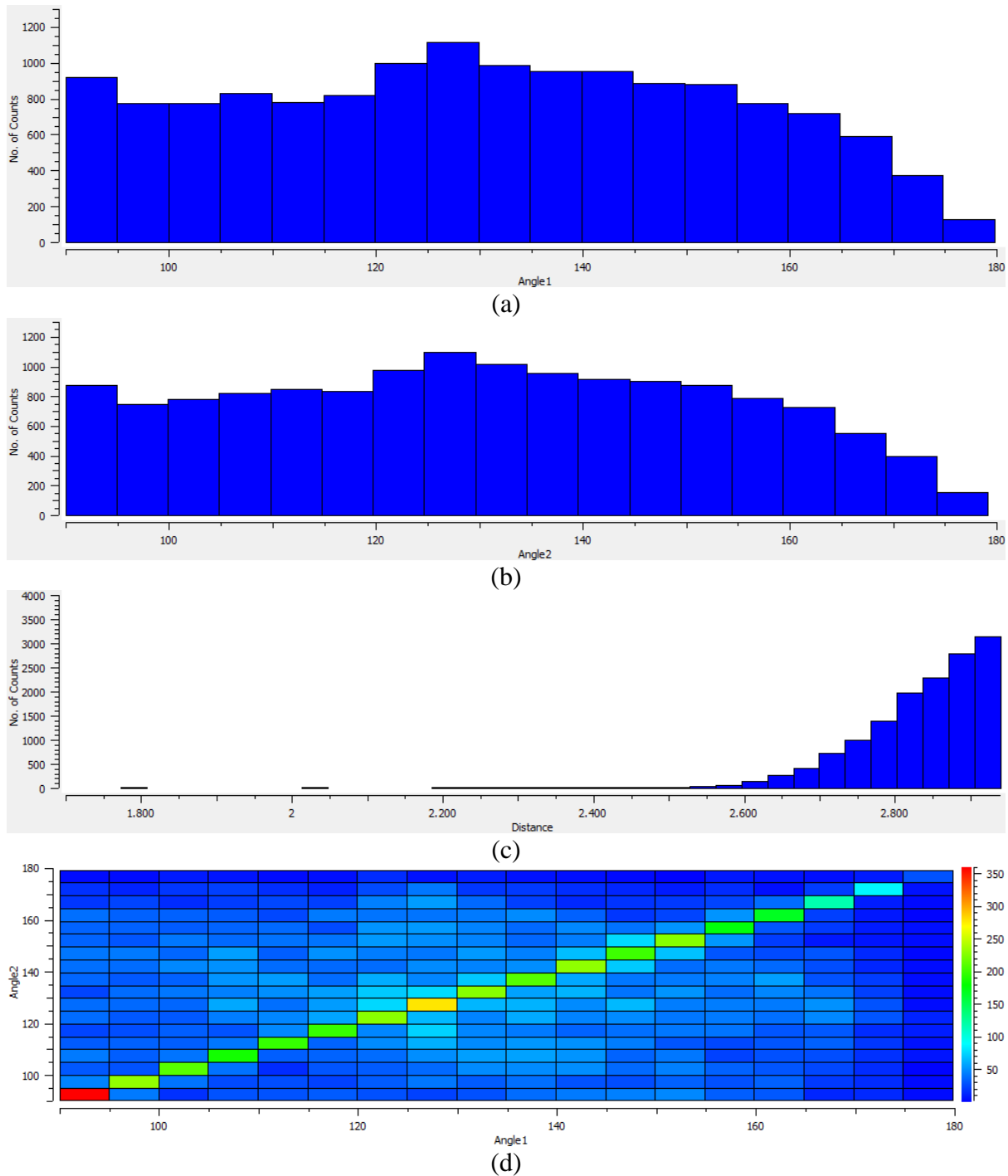


Figure S2: (a) Histogram for angle 1 (θ_1), (b) Histogram for angle 2 (θ_2), (c) Distance histogram, and (d) Heat plot for angle (θ_1 and θ_2), for all the structures having C–F···F–C interaction devoid of strong hydrogen bonding interactions (search 2).

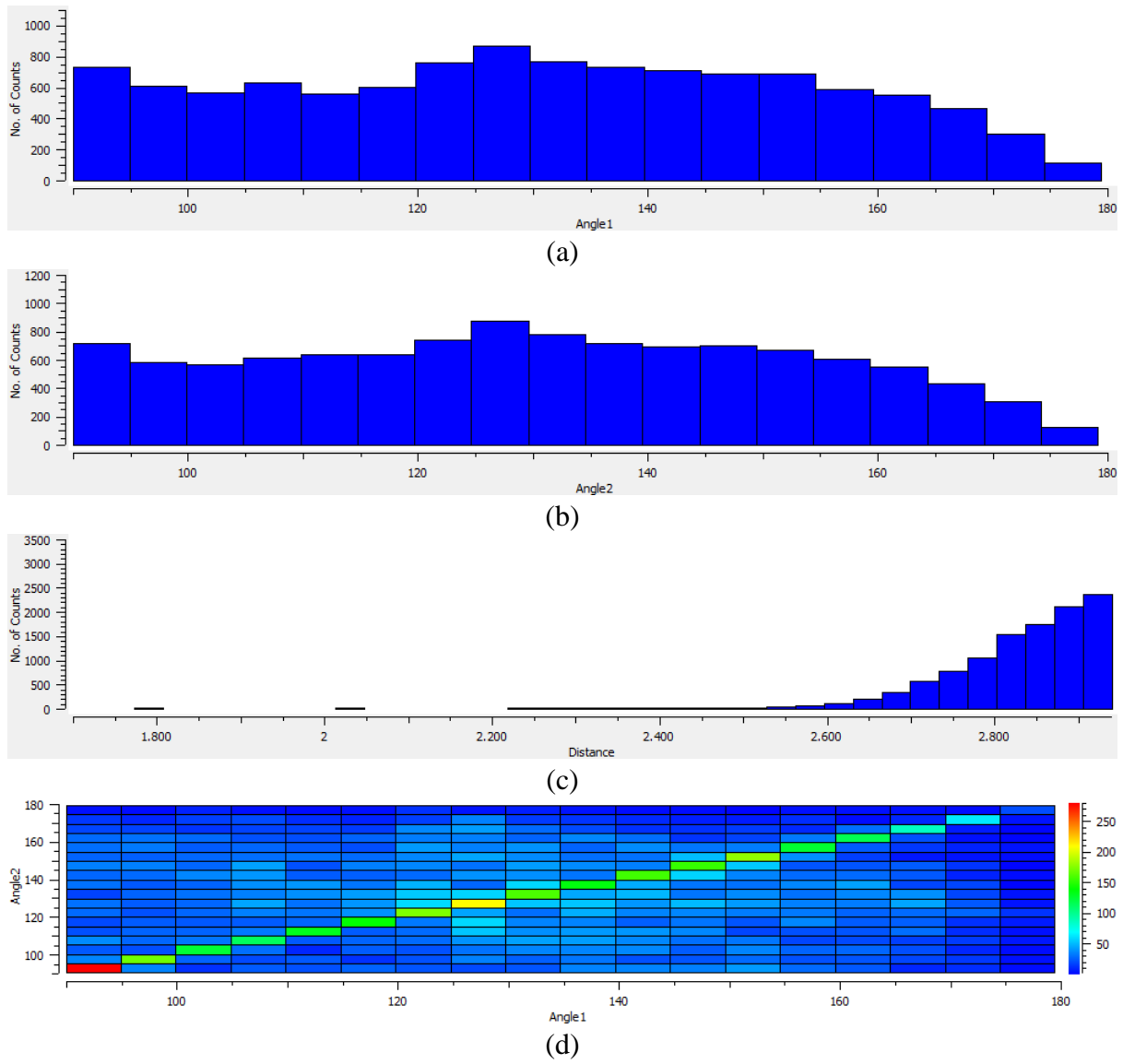
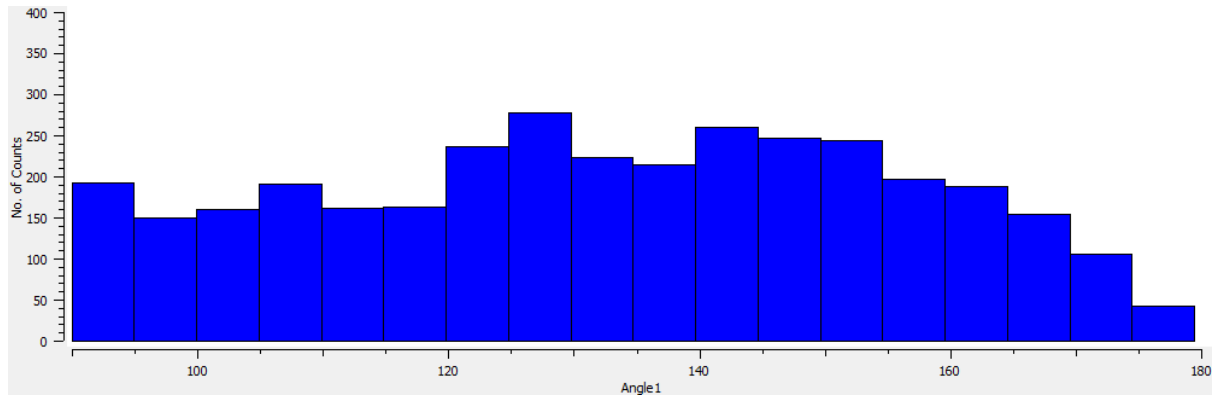
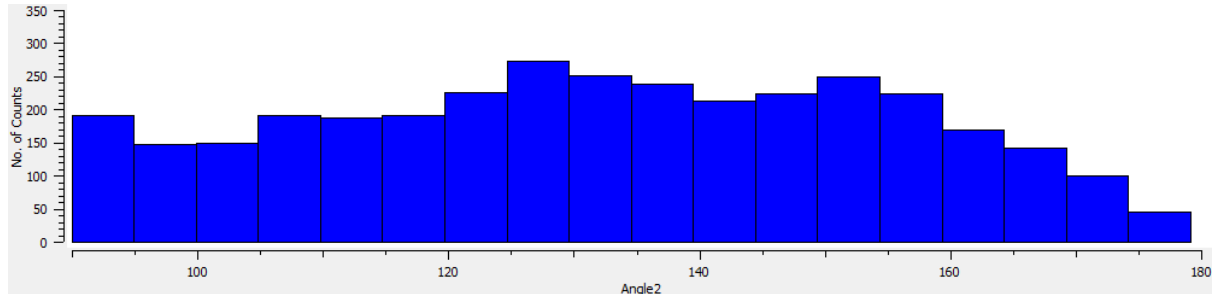


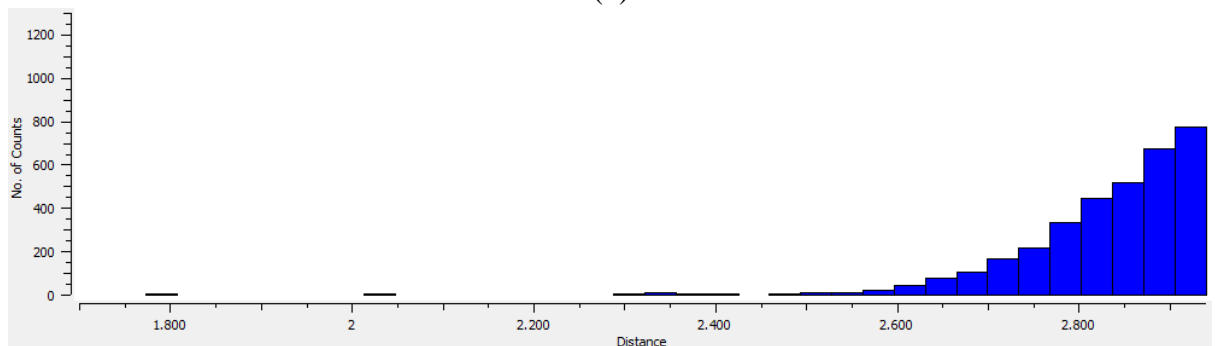
Figure S3: (a) Histogram for angle 1 (θ_1), (b) Histogram for angle 2 (θ_2), (c) Distance histogram, and (d) Heat plot for angle (θ_1 and θ_2), for all the structures having C–F···F–C interaction devoid of strong and weak hydrogen bonding interactions but may contain C–H···F–C interaction (search 3).



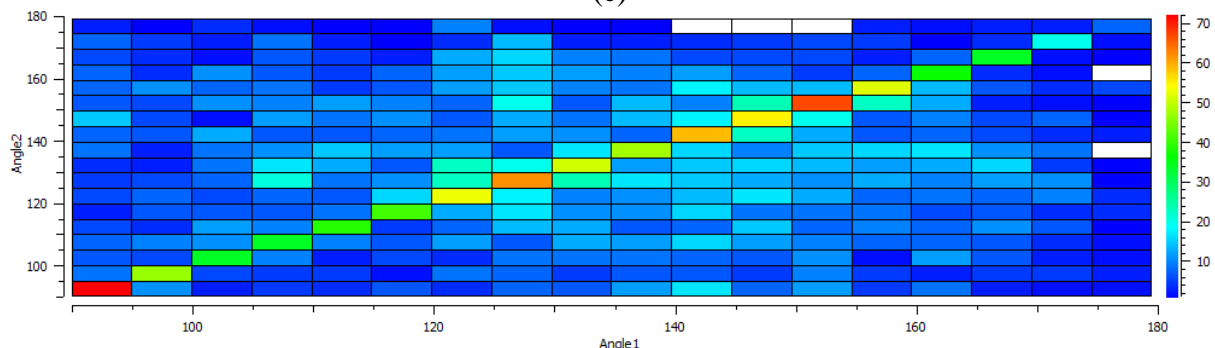
(a)



(b)



(c)



(d)

Figure S4: (a) Histogram for angle 1 (θ_1), (b) Histogram for angle 2 (θ_2), (c) Distance histogram, and (d) Heat plot for angle (θ_1 and θ_2), for all the structures having C–F···F–C interaction devoid of strong and weak hydrogen bonding interactions and not contain C–H···F–C interaction (search 4).

Table S1: Summary of CSD search for C–F···F–C interactions among the structured reported at temperature 80 – 120 K.

Statistical parameters	Search 1	Search 2	Search 3	Search 4
No. of hits	3100	2529	1269	359
No. of interactions	7550	6372	3576	1531
Maximum range for θ_1 (°)	120-135	120-135	120-135	120-160
Maximum range for θ_2 (°)	120-135	120-135	120-135	120-160
Maximum range for distance (Å)	2.90-2.94	2.90-2.94	2.90-2.94	2.90-2.94
No. of type I interactions [0° ≤ θ₁ - θ₂ ≤ 15°]	3583	2958	1593	663
No. of type II interactions [30° ≤ θ₁ - θ₂]	2407	2050	1196	513
No. of quasi type I/type II interactions [15° ≤ θ₁ - θ₂ ≤ 30°]	1560	1364	787	355
Ratio of the number of hits of type I: type II: quasi type I/type II	2.3:1.54:1	2.2:1.50:1	2.02:1.5:1	1.9:1.45:1

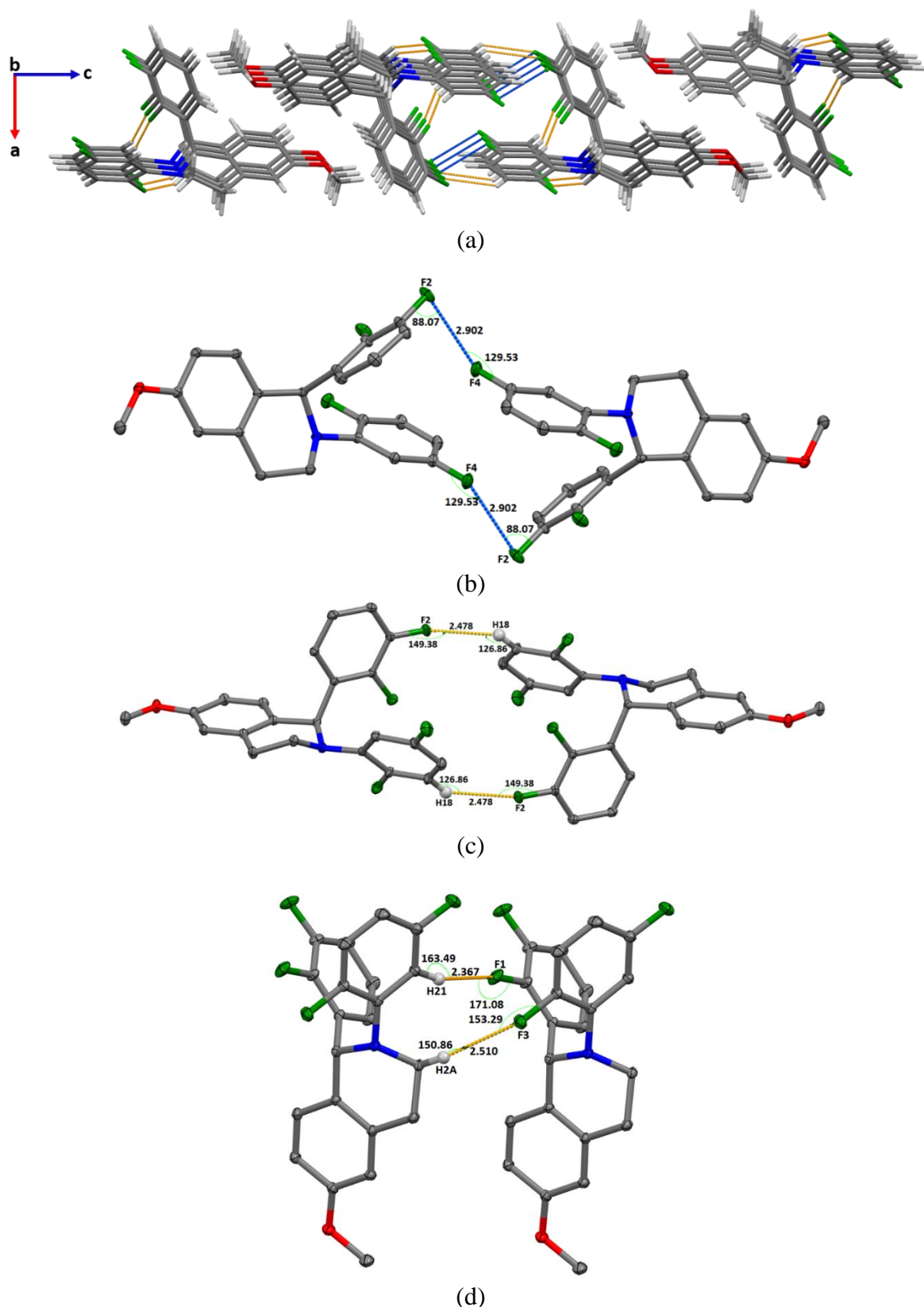


Figure S5: (a) Molecular packing diagram depicting $\text{C}-\text{F}\cdots\text{F}-\text{C}$ interactions (blue dotted lines) and $\text{C}-\text{H}\cdots\text{F}-\text{C}$ hydrogen bonds (orange dotted lines), (b) type II $\text{C}-\text{F}\cdots\text{F}-\text{C}$ intermolecular interaction, (c) intermolecular $\text{C}18-\text{H}18\cdots\text{F}2-\text{C}12$ and, (d) $\text{C}2-\text{H}2\text{A}\cdots\text{F}3-\text{C}13$ and $\text{C}21-\text{H}21\cdots\text{F}1-\text{C}11$ interactions. The distances and angels are given in Å and degrees (°), respectively.

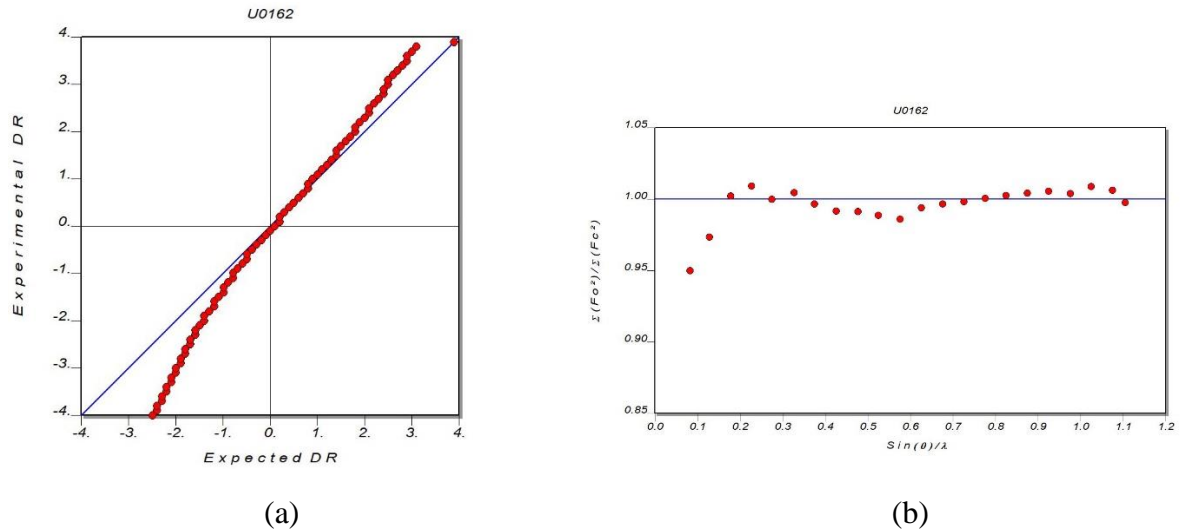


Figure S6: (a) The normal probability distribution plot, (b) Variation of the scale factor with respect to $\sin \theta / \lambda$.

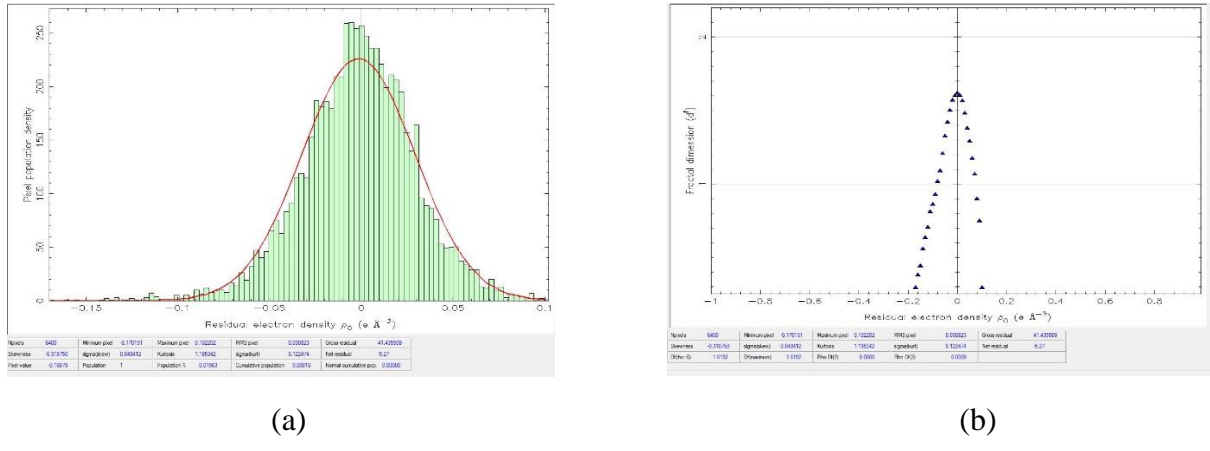


Figure S7: (a) Residual electron density distribution plot, (b) fractal dimension vs residual electron density plot.

Table S2: Atomic charges after final multipole modelling (The values from the experimental and theoretical analyses are given in the first and second rows, respectively).

Atom	Atomic charge	Kappa	Kappa'
F(1)	-0.070	0.997	1.201
	-0.148	0.999	1.201
F(2)	-0.156	0.990	1.196
	-0.159	0.999	1.196
F(3)	-0.171	0.991	1.193
	-0.186	0.996	1.193
F(4)	-0.185	0.989	1.222
	-0.165	0.998	1.222
O(1)	-0.221	0.984	1.211
	-0.143	0.996	1.123
N(1)	-0.137	0.990	0.936
	-0.046	0.993	1.026
C(1)	-0.103	0.996	0.936
	-0.108	0.991	0.903
C(2)	-0.220	0.991	0.938
	-0.302	0.991	0.894
C(3)	-0.182	0.991	0.938
	-0.199	0.991	0.894
C(4)	-0.124	0.994	0.979
	-0.063	0.995	0.852
C(5)	-0.052	0.993	0.933
	-0.076	0.994	0.885
C(6)	-0.143	0.994	0.979
	-0.127	0.995	0.852
C(7)	-0.151	0.994	0.979
	-0.106	0.995	0.852
C(8)	-0.076	0.997	0.948
	-0.097	0.994	0.839
C(9)	-0.030	0.997	0.948
	+0.006	0.994	0.839
C(10)	+0.020	1.006	1.029
	-0.027	0.992	0.833
C(11)	-0.000	1.007	0.987
	+0.003	1.000	0.903
C(12)	+0.116	1.007	0.987
	+0.069	1.000	0.903
C(13)	-0.122	0.994	0.979
	-0.198	0.995	0.852
C(14)	-0.102	0.994	0.979
	-0.218	0.995	0.852
C(15)	-0.192	0.994	0.979
	-0.135	0.995	0.852
C(16)	-0.023	1.001	0.999
	-0.094	0.995	0.885
C(17)	+0.043	1.007	0.987
	+0.017	1.000	0.903
C(18)	-0.197	0.994	0.979
	-0.166	0.995	0.852
C(19)	-0.168	0.994	0.979
	-0.202	0.995	0.852
C(20)	+0.102	1.007	0.987
	-0.022	1.000	0.903
C(21)	-0.222	0.994	0.979
	-0.190	0.995	0.852
C(22)	-0.263	0.990	1.008

	-0.331	0.994	0.890
H(1)	+0.167	1.230	1.230
	+0.208	1.230	1.20
H(2A)	+0.155	1.212	1.212
	+0.193	1.212	1.212
H(2B)	+0.150	1.212	1.212
	+0.174	1.212	1.212
H(3A)	+0.104	1.212	1.212
	+0.172	1.212	1.212
H(3B)	+0.149	1.212	1.212
	+0.188	1.212	1.212
H(4)	+0.187	1.233	1.233
	+0.201	1.233	1.233
H(6)	+0.207	1.233	1.233
	+0.189	1.233	1.233
H(7)	+0.194	1.233	1.233
	+0.183	1.233	1.233
H(13)	+0.199	1.233	1.233
	+0.227	1.233	1.233
H(14)	+0.201	1.233	1.233
	+0.225	1.233	1.233
H(15)	+0.176	1.233	1.233
	+0.201	1.233	1.233
H(18)	+0.237	1.233	1.233
	+0.206	1.233	1.233
H(19)	+0.212	1.233	1.233
	+0.245	1.233	1.233
H(21)	+0.221	1.233	1.233
	+0.192	1.233	1.233
H(22A)	+0.152	1.227	1.227
	+0.222	1.227	1.227
H(22B)	+0.137	1.227	1.227
	+0.203	1.227	1.227
H(22C)	+0.184	1.227	1.227
	+0.186	1.227	1.227

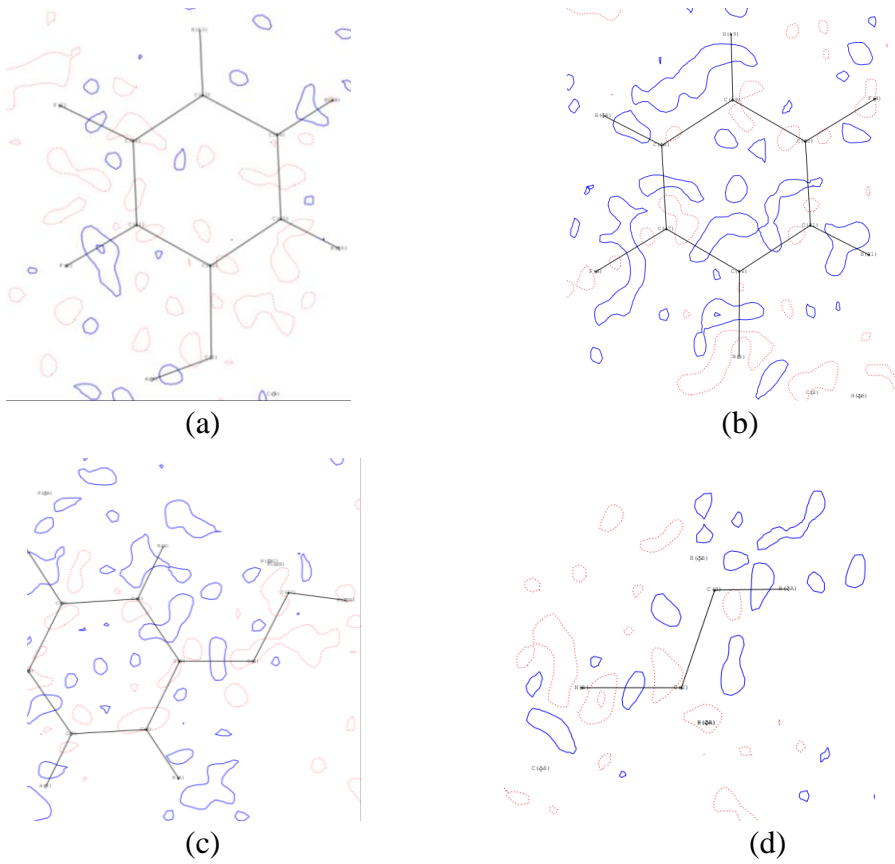


Figure S8: Residual density maps, drawn for the planes having atoms (a) F1, C10, and F2 (b) F3, C16, and F4 (c) C5, O1, and C22 and (d) N1, C2, and C3 using positive (blue, solid line) and negative (red, dotted line) with contour starting at $\pm 0.05 \text{ e } \text{\AA}^{-3}$ and with an interval of $\pm 0.1 \text{ e } \text{\AA}^{-3}$.

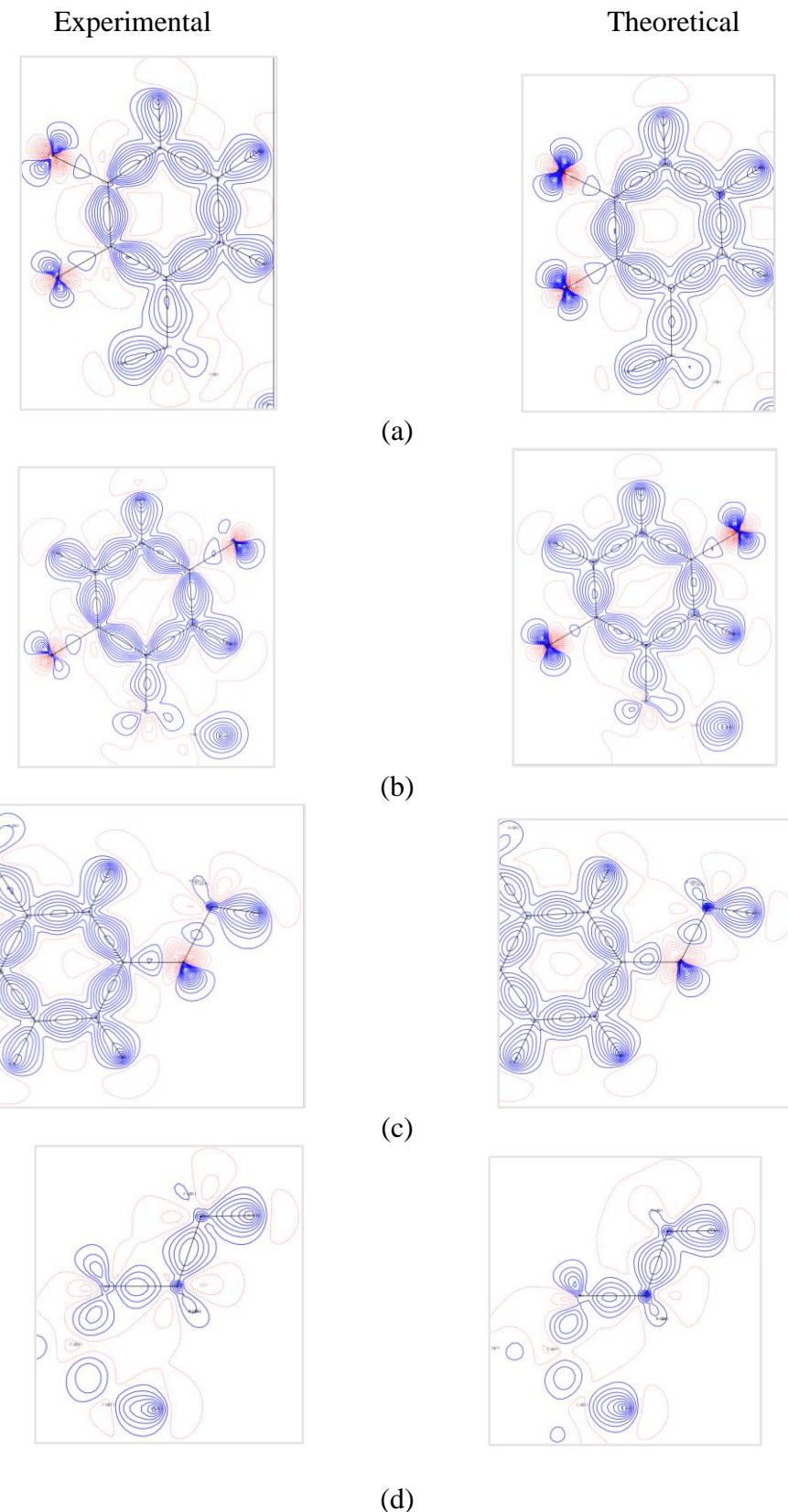
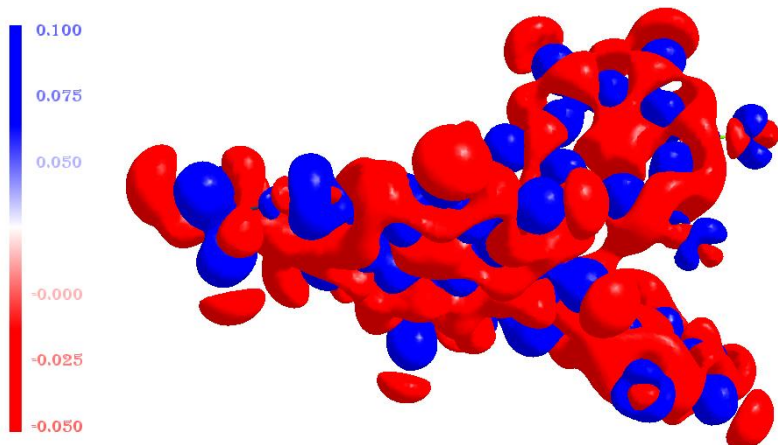
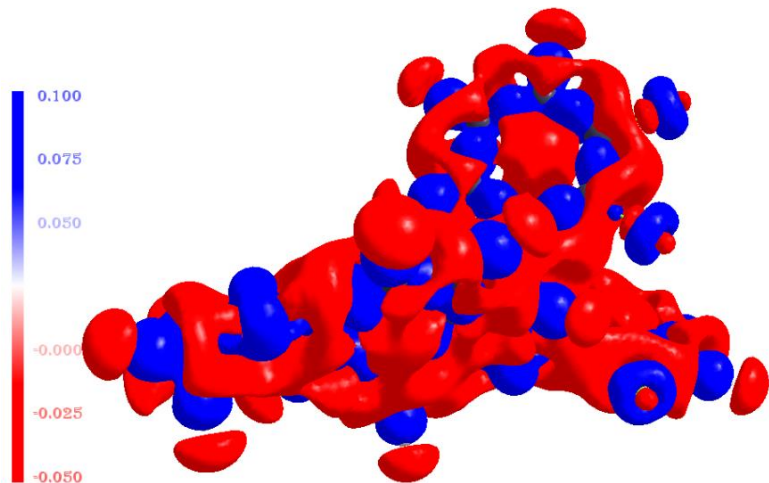


Figure S9: 2D Deformation electron density maps, drawn on the planes containing atoms (a) F1,C10, and F2, (b) F3, C16, and F4, (c) C5, O1, and C22, and (d) N1, C2, and C3 using positive (blue, solid line) and negative (red, dotted line) with contour starting at $\pm 0.05 \text{ e } \text{\AA}^{-3}$ with an interval of $\pm 0.1 \text{ e } \text{\AA}^{-3}$.

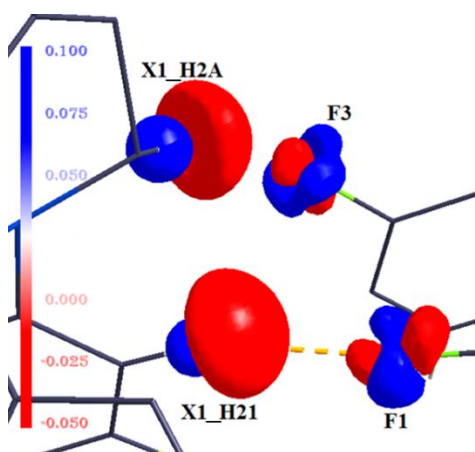


(a)

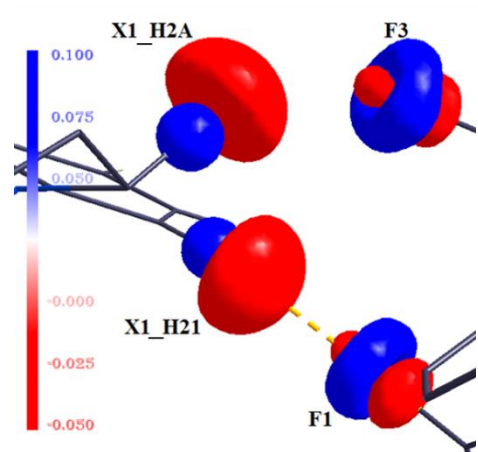


(b)

Figure S10: (a) experimental and (b) theoretical 3D static deformation density maps with positive (blue surface) and negative (red surface).



(a)



(b)

Figure S11: (a) experimental, and (b) theoretical 3D Deformation density maps for the weak C2–H2A···F3–C17 and C21–H21···F1–C11 hydrogen bonds.

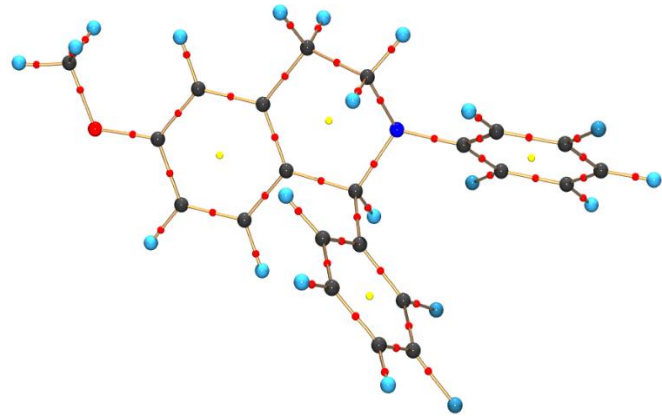


Figure S12: The molgraph view showing BCPs and bond paths for the covalent bonds and the ring critical points.

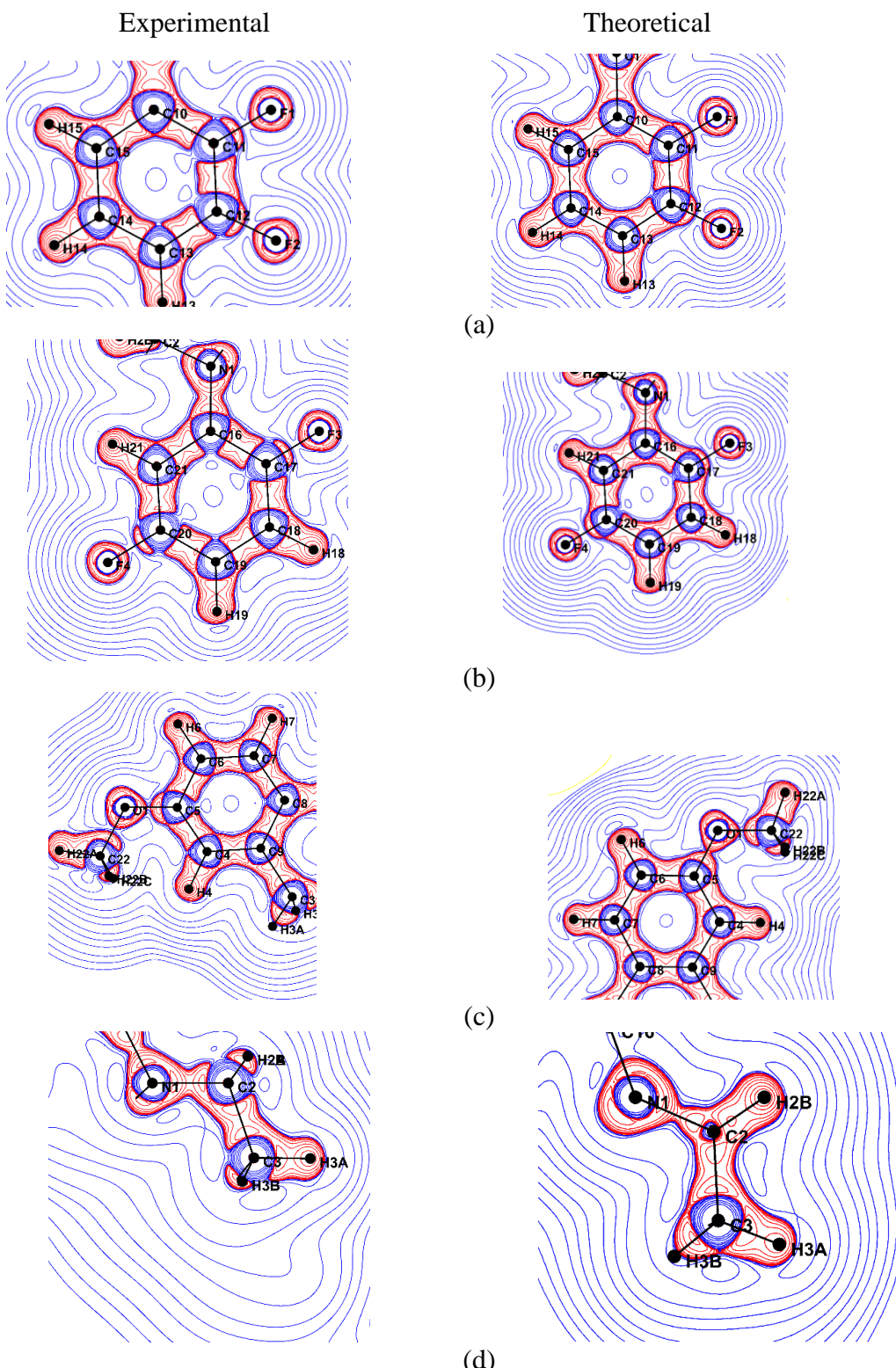


Figure S13: Laplacian ($\nabla^2\rho$) maps on the planes containing atoms (a) F1, C10, and F2, (b) F3, C16, and F4, (c) C5, O1, and C22, and (d) N1, C2, and C3 drawn at the logarithmic interval of $-\nabla^2\rho \text{ e}\text{\AA}^{-5}$.

Table S3: Topological parameters of the covalent bonds in compound **1**. The values from the experimental and theoretical analyses are given in the first and second rows, respectively.

Atom A	Atom B	ρ (eÅ ⁻³)	$\nabla^2 \rho$ (eÅ ⁻⁵)	R _{ij} (Å)	d ₁ (Å)	d ₂ (Å)	λ ₁	λ ₂	λ ₃	ε
F(1)	C(11)	1.875(20)	-16.218(91)	1.347	0.8405	0.5067	-15.47	-14.1	13.35	0.1
		1.899(5)	-15.796(23)	1.347	0.8332	0.5139	-14.85	-14.16	13.22	0.05
F(2)	C(12)	1.855(21)	-14.152(93)	1.341	0.8429	0.4988	-14.48	-13.6	13.93	0.06
		1.887(5)	-15.332(24)	1.342	0.8359	0.5061	-14.41	-14.15	13.22	0.02
F(3)	C(17)	1.761(21)	-12.912(90)	1.357	0.8555	0.5018	-13.9	-12.19	13.17	0.14
		1.784(5)	10.776(22)	1.357	0.8361	0.5214	-12.55	-12.3	14.07	0.02
F(4)	C(20)	1.834(21)	-14.089(97)	1.351	0.8469	0.5044	-14.33	-13.37	13.61	0.07
		1.877(5)	-14.658(23)	1.352	0.8345	0.5176	-14.13	-13.89	13.36	0.02
O(1)	C(5)	1.985(18)	-17.136(88)	1.365	0.8212	0.5444	-15.26	-14.16	12.29	0.08
		2.022(5)	-18.001(23)	1.366	0.8207	0.5454	-15.48	-15.03	12.51	0.03
O(1)	C(22)	1.718(22)	-10.156(91)	1.422	0.8413	0.581	-12.1	-11.1	13.04	0.09
		1.792(5)	-13.524(16)	1.422	0.8352	0.5872	-13.87	-12.94	13.29	0.07
N(1)	C(1)	1.714(14)	-8.781(49)	1.484	0.8222	0.6623	-12.16	-11.20	14.57	0.09
		1.725(4)	-9.943(13)	1.485	0.8192	0.6657	-12.56	-11.56	14.18	0.09
N(1)	C(2)	1.728(15)	-10.255(48)	1.463	0.8315	0.6323	-12.00	-11.35	13.09	0.06
		1.803(4)	-12.873(12)	1.464	0.8254	0.6386	-13.65	-12.54	13.32	0.09
N(1)	C(16)	1.932(21)	-13.811(88)	1.418	0.803	0.6151	-14.55	-13.43	14.17	0.08
		2.012(5)	-16.196(18)	1.417	0.7961	0.6218	-16.21	-13.80	13.81	0.17
C(1)	H(1)	1.842(29)	-16.446(81)	1.099	0.7159	0.3832	-16.88	-16.54	16.98	0.02
		1.847(10)	-17.890(33)	1.099	0.7321	0.3668	-17.55	-17.22	16.87	0.02
C(2)	C(3)	1.647(15)	-10.587(42)	1.520	0.7639	0.757	-10.96	-10.3	10.68	0.06
		1.716(4)	-13.232(9)	1.520	0.7726	0.7483	-11.91	-11.39	10.07	0.05
C(2)	H(2A)	1.812(29)	-15.744(86)	1.093	0.7238	0.3692	-16.85	-16.34	17.45	0.03
		1.871(8)	-19.092(24)	1.092	0.7231	0.3689	-17.87	-17.21	15.99	0.04
C(2)	H(2B)	1.776(30)	-14.764(88)	1.093	0.7234	0.3704	-16.47	-15.88	17.58	0.04
		1.866(8)	-18.254(23)	1.092	0.7253	0.3667	-17.81	-17.09	16.64	0.04
C(3)	H(3A)	1.760(27)	-14.523(71)	1.092	0.6913	0.4008	-15.36	-14.90	15.74	0.03
		1.832(8)	-17.672(24)	1.092	0.7152	0.3768	-16.93	-16.66	15.93	0.02
C(3)	H(3B)	1.736(30)	-14.039(86)	1.092	0.7127	0.3794	-15.63	-15.18	16.77	0.03
		1.859(7)	-19.098(21)	1.092	0.7135	0.3785	-17.40	-17.06	15.35	0.02
C(4)	H(4)	1.772(28)	-15.261(86)	1.083	0.7134	0.3699	-17.13	-15.94	17.82	0.07
		1.855(7)	-17.466(21)	1.083	0.757	0.3773	-17.00	-16.78	16.31	0.01
C(5)	C(4)	2.162(19)	-20.195(53)	1.390	0.715	0.6755	-17.42	-13.05	10.28	0.34
		2.138(4)	-18.955(12)	1.390	0.7406	0.6501	-15.57	-12.83	9.44	0.21
C(5)	C(6)	2.135(19)	-19.278(52)	1.404	0.7239	0.6803	-16.87	-13.00	10.59	0.30
		2.100(4)	-18.793(11)	1.404	0.7261	0.6780	-15.40	-13.09	9.70	0.18
C(6)	H(6)	1.801(29)	-16.374(89)	1.083	0.7180	0.3653	-17.53	-16.59	17.75	0.06
		1.854(6)	-17.519(18)	1.083	0.6923	0.3097	-16.74	-16.37	15.59	0.02
C(7)	C(6)	2.122(18)	-18.518(51)	1.387	0.6937	0.6942	-16.22	-13.13	10.83	0.24
		2.103(3)	-17.632(9)	1.388	0.6769	0.7111	-14.93	-12.45	9.75	0.20
C(7)	H(7)	1.797(28)	-16.023(85)	1.08	0.7152	0.3681	-17.26	-16.57	17.80	0.04
		1.843(7)	-17.017(20)	1.083	0.6961	0.3870	-16.58	-16.42	15.98	0.01
C(8)	C(9)	2.139(22)	-18.375(67)	1.394	0.7029	0.6915	-16.46	-12.91	11.00	0.27
		2.101(4)	-17.824(12)	1.394	0.7077	0.6868	-14.75	-12.62	9.55	0.17

C(8)	C(1)	1.680(15)	-11.124(40)	1.517	0.7664	0.7506	-11.71	-10.52	11.11	0.11
		1.702(3)	-12.244(8)	1.517	0.7567	0.7604	-11.78	-10.72	10.25	0.10
C(8)	C(7)	2.077(18)	-17.718(47)	1.406	0.7063	0.6999	-15.95	-12.82	11.06	0.24
		2.023(3)	-15.757(9)	1.406	0.6959	0.7104	-13.98	-11.89	10.11	0.18
C(9)	C(4)	2.045(17)	-16.878(46)	1.404	0.6992	0.7053	-15.20	-12.60	10.92	0.21
		2.082(3)	-18.293(9)	1.404	0.7087	0.6958	-14.88	-12.96	9.54	0.15
C(9)	C(3)	1.703(15)	-11.171(37)	1.507	0.7552	0.7520	-11.61	-10.76	11.19	0.08
		1.723(3)	-12.700(7)	1.507	0.7557	0.7513	-11.44	-11.42	10.16	0.00
C(10)	C(11)	2.150(24)	-18.532(78)	1.392	0.6581	0.7339	-17.08	-13.42	11.97	0.27
		2.127(4)	-19.080(12)	1.392	0.6583	0.7338	-15.29	-13.22	9.43	0.16
C(10)	C(1)	1.634(17)	-9.421(47)	1.529	0.7724	0.7568	-10.82	-10.58	11.98	0.02
		1.665(3)	-11.563(9)	1.529	0.7634	0.7657	-11.28	-10.51	10.23	0.07
C(10)	C(15)	2.101(22)	-17.179(65)	1.402	0.6973	0.7055	-16.06	-13.28	12.16	0.21
		2.070(4)	-17.604(10)	1.402	0.6946	0.7082	-14.82	-12.38	9.60	0.20
C(11)	C(12)	2.196(21)	-20.308(60)	1.389	0.7027	0.687	-18.46	-13.64	11.79	0.35
		2.246(4)	-22.737(13)	1.390	0.7051	0.6855	-18.07	-18.07	9.77	0.25
C(12)	C(13)	2.223(19)	-21.111(52)	1.380	0.7102	0.6707	-18.01	-14.19	11.09	0.27
		2.194(4)	-19.597(9)	1.381	0.7066	0.6745	-16.30	-13.20	9.900	0.23
C(13)	H(13)	1.813(30)	-16.529(91)	1.083	0.7138	0.3700	-17.54	-16.55	17.57	0.06
		1.837(7)	-17.054(20)	1.083	0.7155	0.3675	-17.31	-16.45	16.71	0.05
C(13)	C(14)	2.075(18)	-17.833(51)	1.396	0.6985	0.6977	-15.86	-12.91	10.94	0.23
		2.080(3)	-17.337(9)	1.396	0.6951	0.7012	-14.70	-12.60	9.96	0.17
C(14)	H(14)	1.793(30)	-15.844(91)	1.083	0.7155	0.3676	-17.38	-16.28	17.81	0.07
		1.887(7)	-18.706(22)	1.083	0.7168	0.3663	-17.83	-17.42	16.42	0.02
C(15)	H(15)	1.824(28)	-16.843(81)	1.083	0.7044	0.3789	-17.34	-16.61	17.10	0.04
		1.883(7)	-18.343(20)	1.083	0.7047	0.3783	-17.77	-16.72	16.15	0.06
C(15)	C(14)	2.093(19)	-18.101(51)	1.394	0.7071	0.6872	-15.98	-13.03	10.90	0.23
		2.100(3)	-17.454(8)	1.394	0.6911	0.7033	-14.80	-12.57	9.91	0.18
C(16)	C(17)	2.171(22)	-19.510(64)	1.400	0.701	0.6994	-18.1	-13.44	12.03	0.35
		2.130(4)	-19.046(13)	1.400	0.6894	0.7114	-16.19	-12.96	10.10	0.25
C(16)	C(21)	2.064(21)	-16.881(58)	1.402	0.7219	0.6802	-16.20	-12.27	11.58	0.32
		2.051(4)	-16.385(12)	1.402	0.7162	0.686	-14.31	-12.32	10.25	0.16
C(17)	C(18)	2.196(18)	-20.541(52)	1.381	0.7268	0.6551	-17.59	-13.68	10.73	0.29
		2.184(4)	-20.391(10)	1.382	0.7173	0.6648	-16.51	-13.44	9.56	0.23
C(18)	C(19)	2.132(18)	-19.126(54)	1.394	0.7059	0.6886	-16.74	-13.37	10.98	0.25
		2.071(3)	-17.005(8)	1.394	0.7073	0.6873	-14.45	-12.58	10.03	0.15
C(18)	H(18)	1.834(30)	-17.382(100)	1.083	0.7337	0.3496	-18.33	-17.54	18.49	0.04
		1.864(7)	-17.577(22)	1.083	0.7079	0.3751	-17.21	-16.77	16.41	0.03
C(19)	H(19)	1.773(28)	-16.178(84)	1.083	0.7092	0.3739	-17.09	-15.96	16.87	0.07
		1.880(7)	-18.800(22)	1.803	0.7225	0.3605	-17.98	-17.45	16.62	0.03
C(20)	C(19)	2.250(19)	-21.230(53)	1.385	0.6703	0.7147	-18.69	-13.95	11.41	0.34
		2.160(4)	-18.587(10)	1.385	0.7217	0.6636	-15.38	-13.25	10.04	0.16

C(21)	C(20)	2.179(18)	-19.743(50)	1.388	0.6594	0.7292	-17.12	-13.63	11.00	0.26
		2.151(4)	-19.025(9)	1.388	0.6683	0.7206	-15.97	-12.95	9.89	0.23
C(21)	H(21)	1.813(30)	-16.225(96)	1.083	0.7282	0.3551	-17.76	-16.95	18.49	0.05
		1.856(7)	-17.247(21)	1.083	0.7033	0.3797	-17.14	-16.51	16.40	0.04
C(22)	H(22A)	1.856(33)	-17.029(97)	1.080	0.7069	0.3731	-17.78	-17.07	17.82	0.04
		1.944(9)	-21.325(28)	1.077	0.7154	0.3616	-19.20	-18.36	16.23	0.05
C(22)	H(22B)	1.856(36)	-16.763(112)	1.077	0.7070	0.3701	-17.80	-17.16	18.20	0.04
		1.945(9)	-20.835(26)	1.077	0.7086	0.3684	-19.10	-17.89	16.15	0.07
C(22)	H(22C)	1.820(35)	-16.501(113)	1.078	0.7222	0.3558	-17.78	-17.32	-18.6	0.03
		1.950(10)	-20.800(30)	1.077	0.7044	0.3727	-18.96	-17.95	16.11	0.06

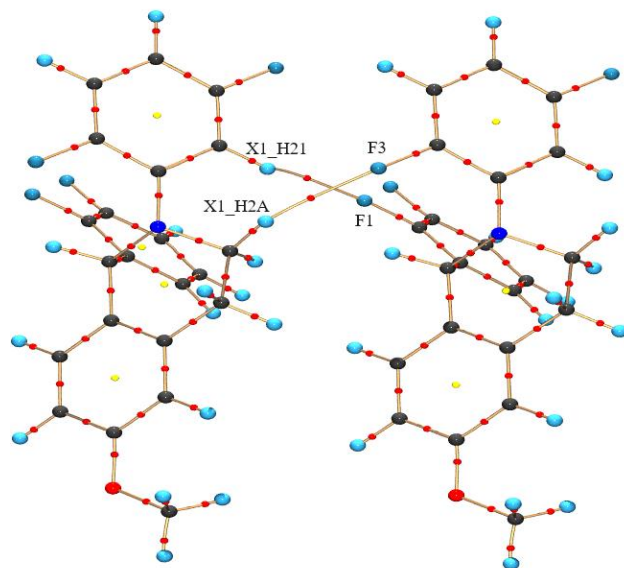
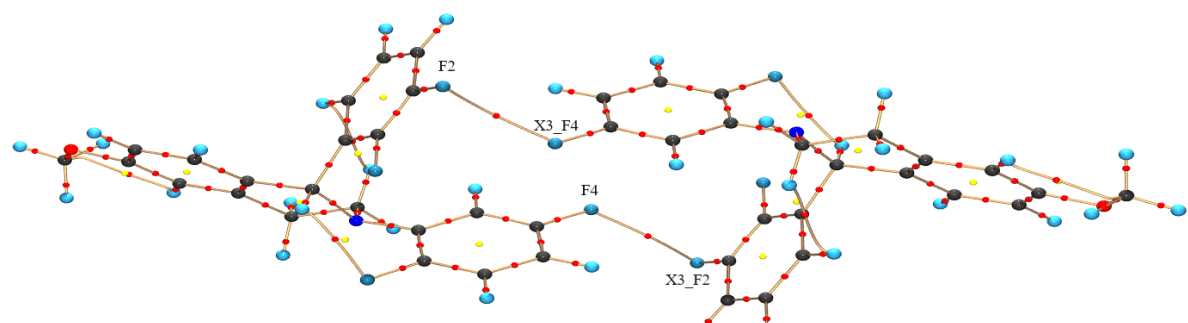
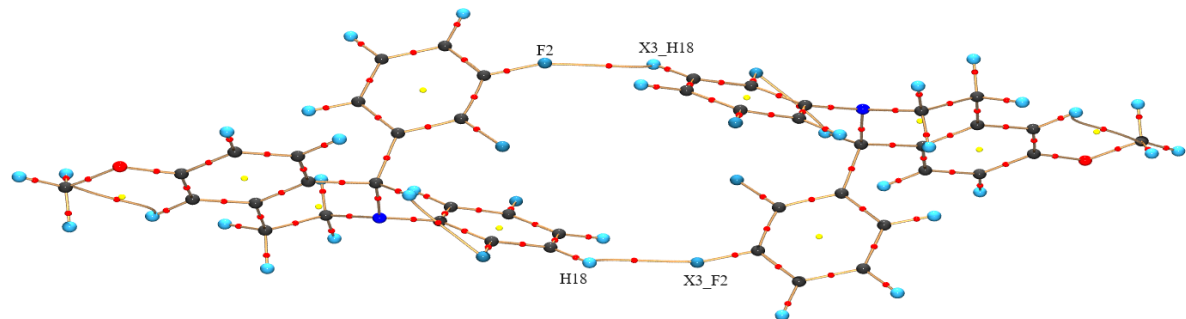


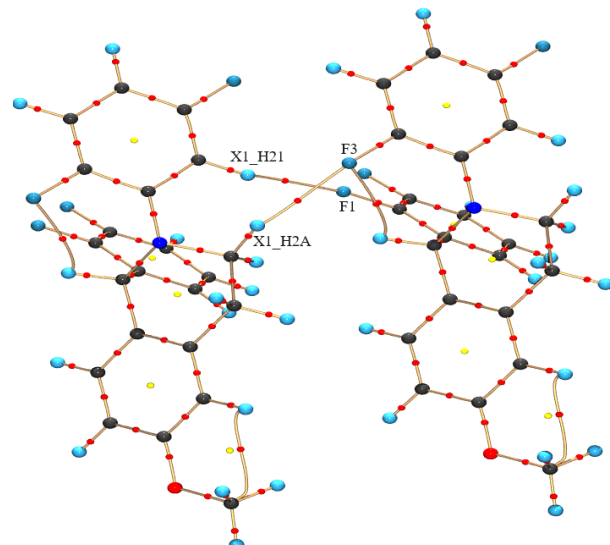
Figure S14: BCPs (red spheres), RCPs (yellow spheres), and bond path (golden line) for the, C21–H21…F1–C11, and C2–H2A…F3–C17 hydrogen bonds based on experimental multipole model.



(a)

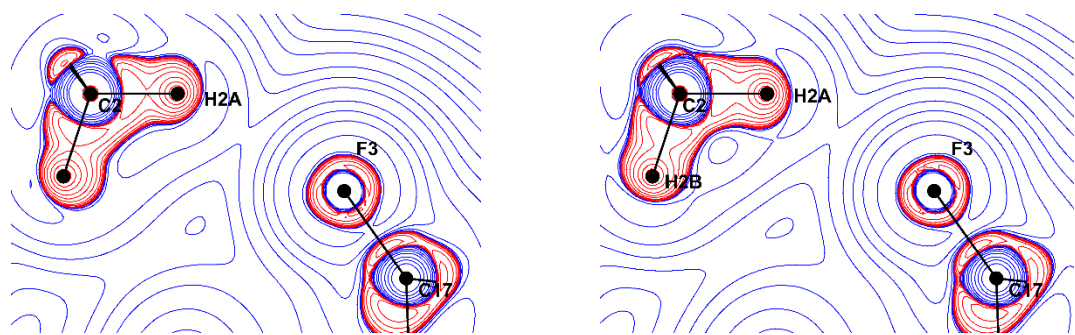


(b)

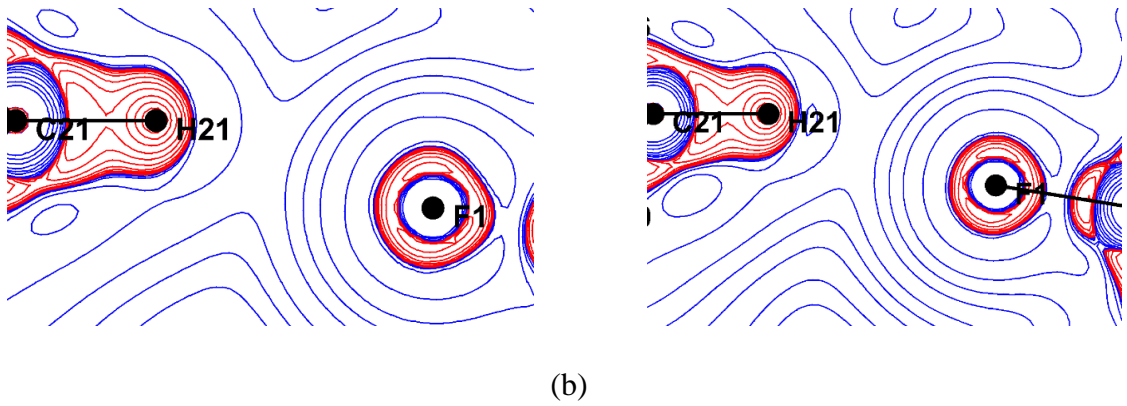


(c)

Figure S15: BCPs (red spheres), RCPs (yellow spheres), and bond path (golden line) for the (a) C12–F2…F4–C20 interaction, (b) C18–H18…F2–C12, (c) C2–H2A…F3–C17, and C21–H21…F1–C11 hydrogen bonds, plotted based on theoretical multipole model.



(a)



(b)

Figure S16: Experimental (left) and theoretical (right) Laplacian maps for (a) C2–H2A…F3–C17 and (b) C21–H21…F1–C11 hydrogen bonds, drawn at the logarithmic interval of $-\nabla^2\rho \text{ e}\text{\AA}^{-5}$.

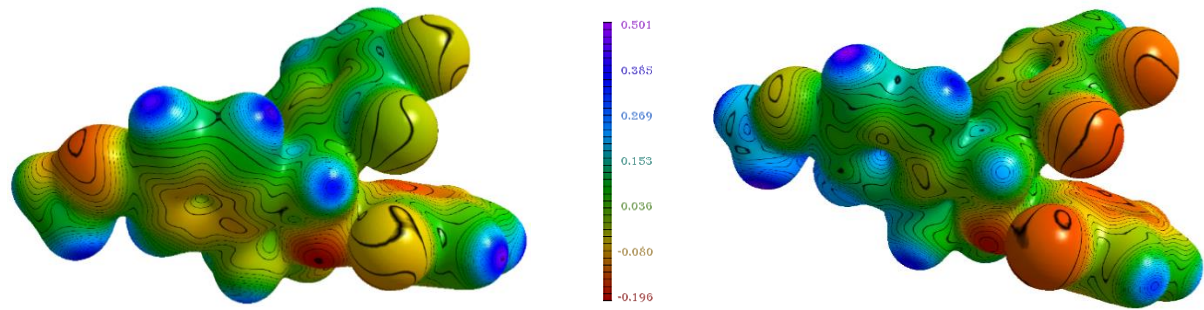


Figure S17: Experimental (left) and theoretical (right) 3D Molecular Electrostatic potential isosurfaces plotted using a same scale.

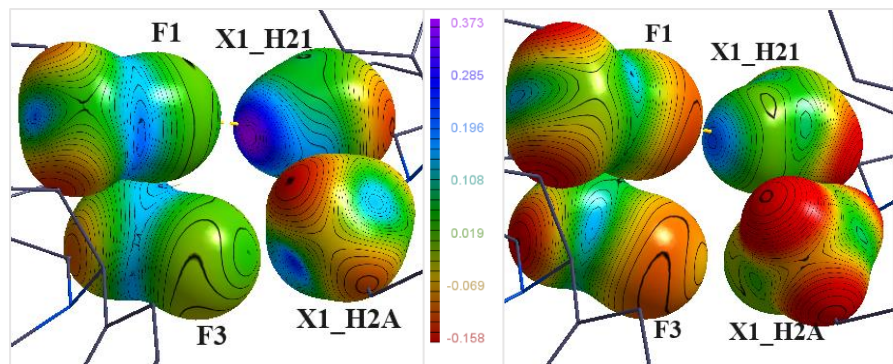


Figure S18: Experimental (left) and theoretical (right) 3D ESP maps for the C21–H21…F1–C11 and C2–H2A…F3–C17 hydrogen bonds.